TU Delft

Delft University of Technology

Influence of Water Content on Shear Strength and Tangential Adhesion Strength of Sand by a Modified Vane Shear Test Device

Chen, Zhongtian; Fang, Yong; Bezuijen, Adam

DOI
10.1061/IJGNAI.GMENG-10366

Publication date
2025

Document Version
Final published version

Published in
International Journal of Geomechanics

Citation (APA)
Chen, Z., Fang, Y., & Bezuijen, A. (2025). Influence of Water Content on Shear Strength and Tangential Adhesion Strength of Sand by a Modified Vane Shear Test Device. *International Journal of Geomechanics*, *25*(2), Article 04024341. https://doi.org/10.1061/IJGNAI.GMENG-10366

Important note
To cite this publication, please use the final published version (if applicable).
Please check the document version above.

Copyright
Other than for strictly personal use, it is not permitted to download, forward or distribute the text or part of it, without the consent of the author(s) and/or copyright holder(s), unless the work is under an open content license such as Creative Commons.

Takedown policy
Please contact us and provide details if you believe this document breaches copyrights.
We will remove access to the work immediately and investigate your claim.

This work is downloaded from Delft University of Technology.
For technical reasons the number of authors shown on this cover page is limited to a maximum of 10.

Green Open Access added to TU Delft Institutional Repository

'You share, we take care!' - Taverne project

https://www.openaccess.nl/en/you-share-we-take-care

Otherwise as indicated in the copyright section: the publisher is the copyright holder of this work and the author uses the Dutch legislation to make this work public.

Check for updates

Influence of Water Content on Shear Strength and Tangential Adhesion Strength of Sand by a Modified Vane Shear Test Device

Zhongtian Chen[1]; Yong Fang[2]; and Adam Bezuijen[3]

Downloaded from ascelibrary.org by Technische Universiteit Delft on 12/23/24. Copyright ASCE. For personal use only; all rights reserved.

Abstract: The shear strength of sand is important to the design and modeling of shield tunneling, and the tangential adhesion strength is a key parameter when determining the pressure gradient along the screw conveyor, the clogging of soil, and the abrasion of the cutting tools. This paper brings up an accurate vane and plate shear test device, which could increase the accuracy of measurements by quantifying and eliminating the influence of torque fluctuation. The peak and residual values of the shear strength and tangential adhesion strength are measured at atmospheric pressure, with water contents from 0% to 25%, and rotation speeds from 0 to 5 r/min. The test results demonstrate that the peak values increase to a maximum value and then decrease with water content. The water content that corresponds to the maximum peak value was between 5% and 20%; the finer the sand, the higher the water content. The ratio between the tangential adhesion strength and shear strength (ratio α) decreases with water content, from approximately 0.7 at a water content of 0% to approximatley 0.4 at 25%. The vane shear test reaches a peak value within 0.17 rotations, and the plate shear test reaches a peak value between 0.25 and 0.55 rotations. Both tests reach residual values after five full rotations. In addition, finer sands have higher shear strengths and higher ratio α.
DOI: 10.1061/IJGNAI.GMENG-10366. *© 2024 American Society of Civil Engineers*.

Author keywords: Laboratory test; Sand; Shear strength; Shield tunneling; Tangential adhesion strength.

Introduction

The shear and tangential adhesion strengths between soil and metal play important roles during shield tunneling. The shear strength is crucial in the numerical simulation and construction of shield tunneling (Broms and Bennermark 1967; Wilson et al. 2013; Ukritchon et al. 2017; Zhang et al. 2020; Chen et al. 2022a; Shi et al. 2023; Wang et al. 2023; Xiao et al. 2023). Reasonable tangential adhesion strength between soil and metal helps to reduce tool abrasion by reducing friction (Gharahbagh et al. 2011; Rostami et al. 2012; Gharahbagh et al. 2013; Gharahbagh et al. 2014; Tang et al. 2022; Ke et al. 2023), reduces clogging at the cutterhead by reducing adhesion and removing soil that is stuck (Feinendegen et al. 2010; Zumsteg et al. 2013; Barzegari et al. 2020; Avunduk et al. 2021; Chen et al. 2022b), makes the tunnel face pressure control more accurate by reducing pressure asymmetry (Bezuijen et al. 2006; Bezuijen and Talmon 2014; Wang et al. 2019; Bezuijen et al. 2022), and allows a sufficient pressure gradient to be established along the screw conveyor (Talmon and Bezuijen 2006; Merritt and Mair 2008).

The laboratory vane shear test is widely adopted to measure the undrained shear strength based on the assumption that the cylindrical yield surface is equal to the surface described by the vane diameter (Dzuy and Boger 1985; ASTM D4648, ASTM 2016), the undrained shear strength can be calculated by the following equation:

$$\tau_v = \frac{T_v}{\pi d_v^2 \left(\frac{h_v}{2} + \frac{d_v}{6}\right)} \tag{1}$$

where τ_v = undrained shear strength; T_v = torque measured by the vane; d_v = diameter of the vane; and h_v = height of the vane. Meng et al. (2011) found that the shear strength of sand increased with the confining pressure. Mori et al. (2018) demonstrated that the shear strength increases linearly with the effective stress. Yang et al. (2018) indicated that the torque that is measured by the vane shear test device increases with the shear rate. Lee et al. (2022) found that the yield stress of vane shear tests correlated with slump tests. Zhong et al. (2023) found that peak shear strength is not sensitive to shear rate when no vertical effective stress exists.

The laboratory plate shear test, which is designed based on the laboratory vane shear test device, is used to measure the tangential adhesion strength between soil and metal. The tangential adhesion strength is calculated by the following equation:

$$\tau_p = \frac{6T_p}{\pi d_p^3} \tag{2}$$

where τ_p = tangential adhesion strength; T_p = torque measured by the plate; and d_p = diameter of the plate. Previous plate shear tests were mainly performed with clay. Peila et al. (2016) performed plate shear tests in foam-conditioned clay and found that

[1]Postdoctoral Researcher, Dept. of Civil Engineering, Southwest Jiaotong Univ., Key Laboratory of Transportation Tunnel Engineering of Ministry of Education, Chengdu 610031, China; Dept. of Civil Engineering, Ghent Univ., Laboratory of Geotechnics, Technologiepark 68, Ghent 9052, Belgium (corresponding author). ORCID: https://orcid.org/0000-0002-8273-1696. Email: zhongtian.chen@ugent.be

[2]Professor, Dept. of Civil Engineering, Southwest Jiaotong Univ., Key Laboratory of Transportation Tunnel Engineering of Ministry of Education, Chengdu 610031, China. Email: fy980220@home.swjtu.edu.cn

[3]Professor, Dept. of Civil Engineering, Ghent Univ., Laboratory of Geotechnics, Technologiepark 905, Ghent 9052, Belgium; Deltares, Dept. of Civil Engineering, Geo-Engineering, P.O Box 177, Delft 2600 MH, the Netherlands. Email: adam.bezuijen@ugent.be

Note. This manuscript was submitted on March 4, 2024; approved on August 26, 2024; published online on November 29, 2024. Discussion period open until April 29, 2025; separate discussions must be submitted for individual papers. This paper is part of the ***International Journal of Geomechanics***, © ASCE, ISSN 1532-3641.

a foaming agent with the polymer works better at reducing the torque measured. Wang et al. (2020) found that the tangential adhesion strength reduces with a dispersant injection when the concentration is lower than 4%. Wang et al. (2022) demonstrated that soil particles smaller than 0.15 mm is crucial to clogging.

In mathematical screw conveyor pressure gradient models, the shear strengths on the casing of the screw conveyor (τ_c), screw shaft (τ_s), and screw flight surfaces (τ_f) are of vital importance (Merritt and Mair 2008; Talmon and Bezuijen 2006). Merritt and Mair (2008) found that the shear strength on the casing is approximately equal to the undrained shear strength (s_u) of the discharged soil, τ_s and τ_f are assumed to be equal, and a screw casing shear strength ratio (α) is defined as follows:

$$\alpha = \frac{\tau_f}{\tau_c} = \frac{\tau_s}{\tau_c} \tag{3}$$

Zumsteg and Puzrin (2012) studied the influence of the surfactant and polymer on ratio α by taking the tangential adhesion strength as τ_s and τ_f; the ratio decreased in conditioned illite, increased in conditioned bentonite and remained relatively stable in conditioned kaolin. They concluded that the clay mineral type has a significant influence on the ratio α. Zumsteg et al. (2013) performed extra tests with amines-conditioned soil and observed that amines could reduce the tangential adhesion strength. The shear strength of the conditioned illite remained constant, which resulted in a reduction of the ratio α.

In shield tunneling areas, many laboratory vane and plate shear tests were performed, which provide valuable data for the evaluation of clogging and soil strength (Mori et al. 2018; Wang et al. 2020). However, the comparison between the results of vane and plate shear tests in sand is seldom studied, although this comparison could be very important in the abrasion of cutting device and the pressure gradient along the screw conveyor (Merritt and Mair 2008; Rostami et al. 2012). In a screw conveyor, the soil pressure is likely to drop to zero at the outlet to enable a fluent soil discharge (Bezuijen et al. 2006; Vinai et al. 2008). However, most laboratory vane and plate shear tests are performed with a confining pressure applied, and a certain knowledge gap exists on soil behavior under atmospheric pressure. During the pressurized vane shear test (Lee et al. 2022) and pressurized plate shear test (Peila et al. 2016; Liu et al. 2019; Wang et al. 2020), fluctuations exist. In pressurized tests, this fluctuation has a limited influence on test results and could even be neglected, because the fluctuation is reasonably small compared with the value being measured. However, in tests at atmospheric pressure, relatively large fluctuations reported in the pressurized tests are no longer acceptable, because the value being measured is quite small.

To solve this measurement accuracy problem and partly address the current knowledge gap, this paper presents a laboratory vane and plate shear test device, which could increase the accuracy of the measurements by quantifying and eliminating the influence of torque fluctuation. The peak and residual values of the shear and tangential adhesion strengths are measured with accuracy at atmospheric pressure. The ratio between the tangential adhesion strength and shear strength (ratio α) in sand is studied, which is not well reported to date. The results are believed to have a wider application range, because the mineral content of sand is much simpler than that of clay.

Methodology

Experimental Setup

The test apparatus in this paper could be used to measure the undrained shear strength and tangential adhesion strength between sand and metal, as shown in Fig. 1. The test apparatus consisted of a motor, torque sensor and monitor, loading frame, motor control, pressure signal collector, and soil container. The soil container was a steel cylinder with an inner diameter of 200 mm and a height of 235 mm. The bottom plate of the soil container had a circular opening for placing the vane and plate shaft. The steel vane had a diameter of 50 mm and a height of 50 mm, and the steel plate had a diameter of 80 mm. The initial positions of the vane and the plate shear device during the test are shown in Fig. 1. The vane and plate shear device were connected to shafts, and the shaft could be installed to the torque sensor by a connector. The torque sensor in the test apparatus has a range of 10 N·m and an accuracy of 0.1%, and the torque was recorded at 1 Hz. The undrained shear strength and tangential adhesion strength were calculated by Eqs. (1) and (2), respectively. A hammer with a diameter of 50 mm was used to fill the soil sample to the soil container, as shown in Fig. 1. The hammer standardized the impact by freefalling the weight of 1.25 kg from 150 mm.

Sample Preparation

The grain size distributions of sands that were tested in this paper are shown in Fig. 2. Some geotechnical properties of the tested sands were tested following GB/T 50123 (MHURD 2019); the

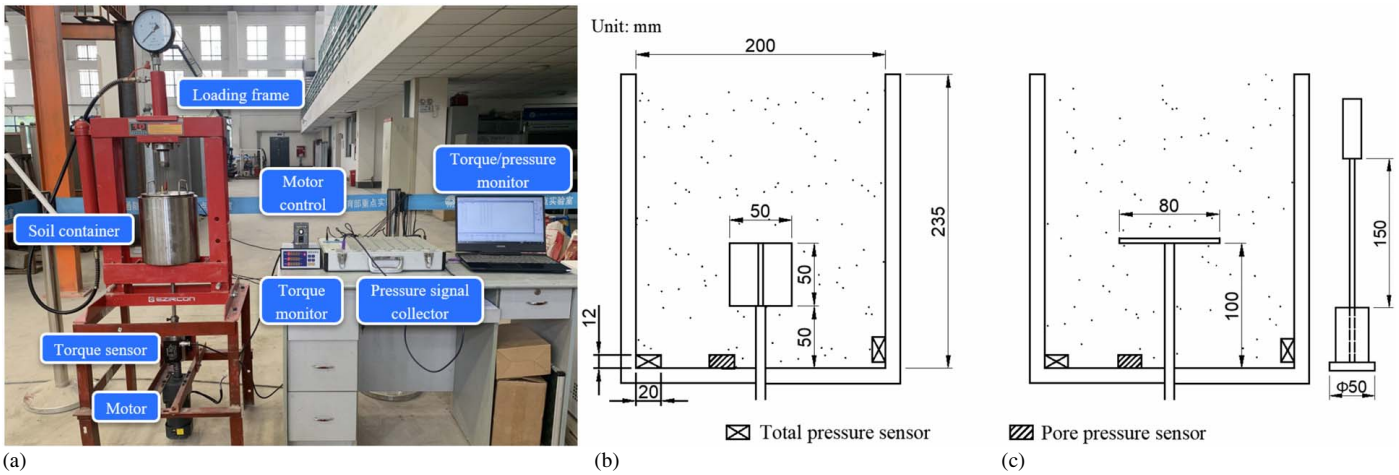

Fig. 1. Showing: (a) test apparatus for vane and plate shear tests: (b) the soil container; and (c) the hammer to fill the soil container. Units = mm.

Downloaded from ascelibrary.org by Technische Universiteit Delft on 12/23/24. Copyright ASCE. For personal use only; all rights reserved.

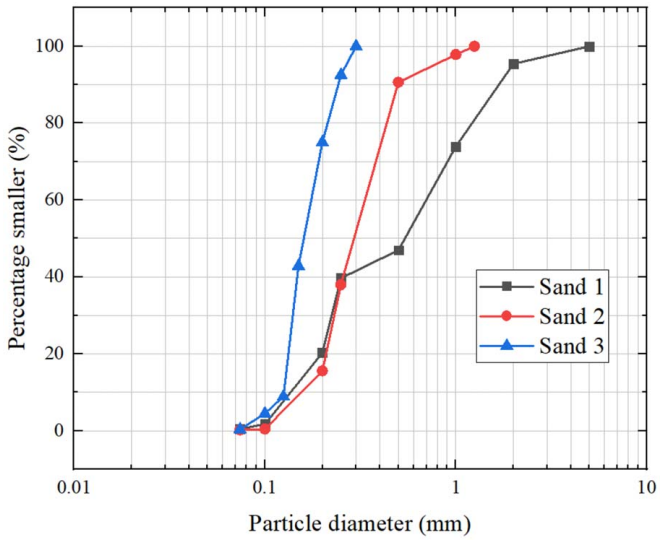

Fig. 2. Grain size distribution curves of tested sands.

data is listed in Table 1. The tested sands were first placed in an oven at 100°C for 24 h to remove any water inside the sand. The dry sand particles were mixed for 2 min and water was added to the dry sand and mixed for another 2 min to reach the desired water content.

Test Procedures

The vane and plate shear tests were performed following the test procedures listed as follows.

1. Prepare the sands with the desired water content described in the previous section.
2. Install the vane and plate shear device. The vane was fixed in a vertical direction, and the plate could move vertically to allow close interactions between the sand and the plate shear device. The initial positions of the two devices are shown in Fig. 1.
3. Fill the container with four layers. The first three layers were hammered 30 times, and the final layer was hammered 50 times. After the sample has been filled and leveled, fix the plate in the vertical direction with a screw that was installed on the shaft.
4. Start the test with the desired rotation speed and record the torque at 1 Hz. The test ended after 10 rotations of the vane or the plate shear device. The shear and tangential adhesion strengths using Eqs. (1) and (2) were calculated, respectively.

Test Groups

The parameters that were changed in the tests in this paper are listed in Table 2. In the plate and vane shear tests, water contents were selected in the range of 0%–5%, with 5% as an interval. The maximum water content was 25%, because all three sands became saturated at this value. Therefore, the water content selection could cover the scenarios from the tunneling above the water level to the tunneling below the water level. The rotation speeds during

Table 1. Geotechnical properties of tested sands

Soil properties	Soil 1	Soil 2	Soil 3
Specific gravity (G_s)	2.63	2.65	2.64
e_{max}	0.62	0.80	0.89

Note: e_{max} = Maximum void ratio.

Table 2. Parameters changed in the tests in this paper

Test types	Sand samples	Water content (%)	Rotation speeds (r/min)
Vane and plate shear tests	Sands 1, 2, and 3	0, 5, 10, 15, 20, and 25	1, 2, 3, 4, and 5

the plate and vane shear tests were between 1 and 5 r/min, with 1 r/min as an interval. The lowest and highest values of 1 and 5 r/min were selected, because they were in the typical rotation speed range of the cutterhead and screw conveyor, respectively. The selection of the rotation speed makes test results from this paper useful in the study of the cutterhead and screw conveyor.

Initial Tests and Calibration

To ensure the accuracy of tests in this paper, the fluctuations in the measured torque should be strictly controlled. To minimize the fluctuations, calibration tests were performed in air, foam, water, and some random sand samples. The test procedures for the calibration tests in air, foam, and water followed the description in the section "Test Procedures," except that the plate could be fixed in the vertical direction in Step 2, and the hammer was not needed when filling the container.

The torque fluctuation that was measured with the test apparatus in this paper when conducting the tests in air is shown in Fig. 3. Similar fluctuations could be observed with each turn of the shear device. The highest torque in one rotation was defined as the high value and the lowest torque as the low value; Fig. 3 shows that the peak high value of the measured torque curve in air was 0.06 N·m, and the peak low value was 0.01 N·m.

To obtain data with accuracy and study the influence of rotation speed, the fluctuations in tests with various rotation speeds should be tested, and the test results should be calibrated. Tests at various rotation speeds were carried out in the air, and the torque fluctuations against rotation speeds are shown in Fig. 4. This figure shows that the fluctuation range remained constant despite the change in rotation speed; the peak high and peak low values were 0.06 and 0.01 N·m.

More calibration tests were carried out with air and foam as the test materials. The torque fluctuation values of the plate shear tests

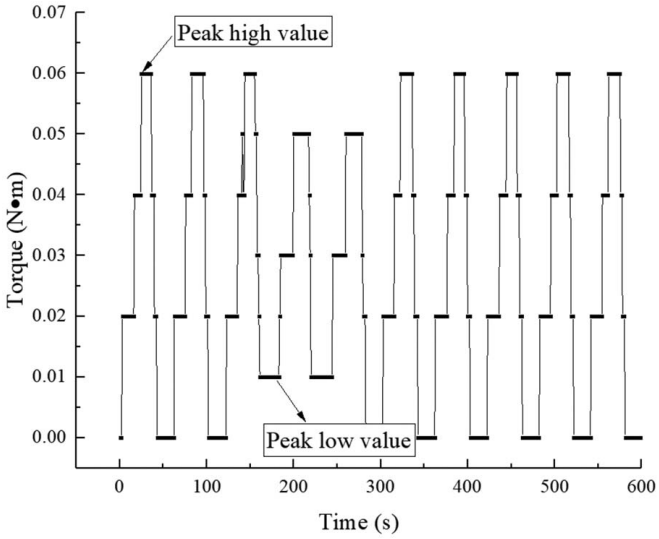

Fig. 3. Torque fluctuation curve in air with rotation speed 1 r/min.

Downloaded from ascelibrary.org by Technische Universiteit Delft on 12/23/24. Copyright ASCE. For personal use only; all rights reserved.

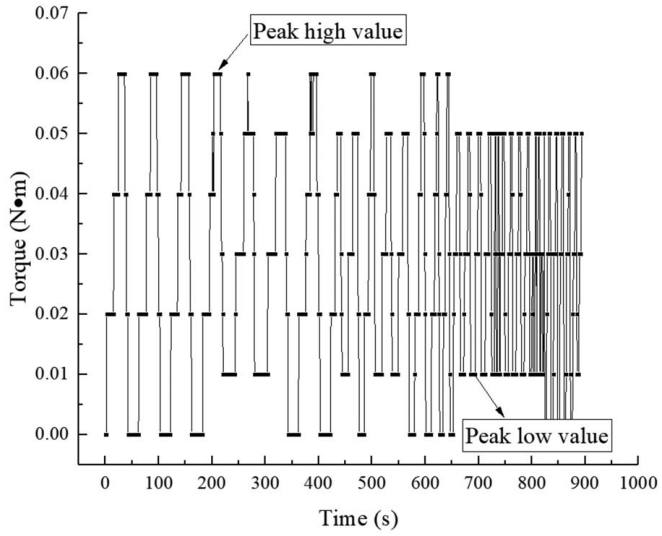

Fig. 4. Torque fluctuation of tests in air with various rotation speeds.

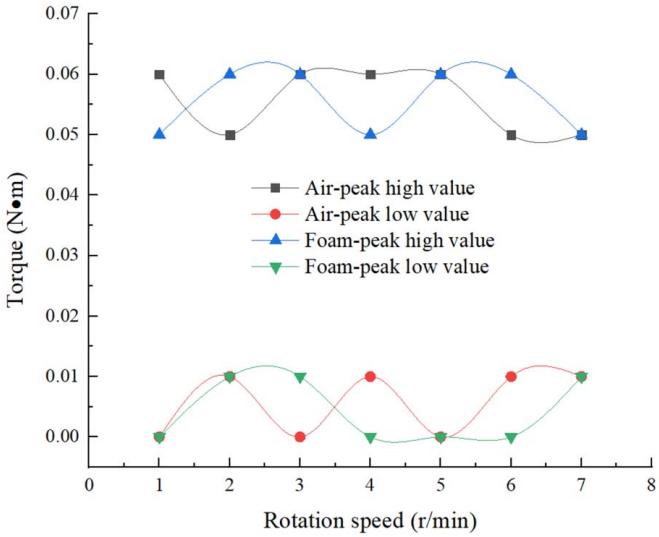

Fig. 5. Peak high and peak low values of torque fluctuation of plate shear tests in air and foam with various rotation speeds.

against rotation speeds are shown in Fig. 5. This figure shows that the fluctuations remained quite stable despite the change in rotation speed and test material. The peak high value was between 0.05 and 0.06 N·m, and the peak low value was between 0 and 0.01 N·m. The change in rotation speed had a very limited influence on the fluctuation; the test results that were performed with sands under various rotation speeds were not influenced by the change in fluctuation that was caused by the rotation speed change. In addition, most of the low values were 0 N·m, and the peak low values remained at a very low value, which agreed with the zero-shear resistance hypothesis for tests in air; the low value measured could be considered the actual value. Therefore, the torque curve during the tests could be obtained by subtracting the fluctuation curve (which will appear with the residual shear strength) from the recorded torque curve. The fluctuation in the vane and plate shear tests were the same, because they shared the same sealing system and motor.

The typical torque curves for the plate and vane shear tests are shown in Fig. 6, which were obtained in tests with a rotation speed of 5 r/min in random sand. After the measured torque value was relatively stabilized, by taking the torque in one random rotation as the standard fluctuation and repeating it for the test process, the fluctuation curves could be determined. This shows that the torque fluctuation increased to 0.5 N·m due to the increased resistance during tests in the sand. The calibration was performed by subtracting the fluctuation curve from the recorded torque curve; the residual torque value was taken as the average torque value after five rotations. Of note, the accuracy of this calibration could only be guaranteed when the low value in the increased fluctuation curve represented the actual torque. To verify the accuracy of this calibration, a torque wrench with a range of 5 N·m, with an accuracy of 0.1 N·m, was used to measure the peak torque of the plate and vane shear tests; the tested values are shown in Fig. 6. This figure shows that the values that were measured by the torque wrench were quite close to the calibrated peak values of the torque curves, which indicated that the accuracy of the calibration could be guaranteed.

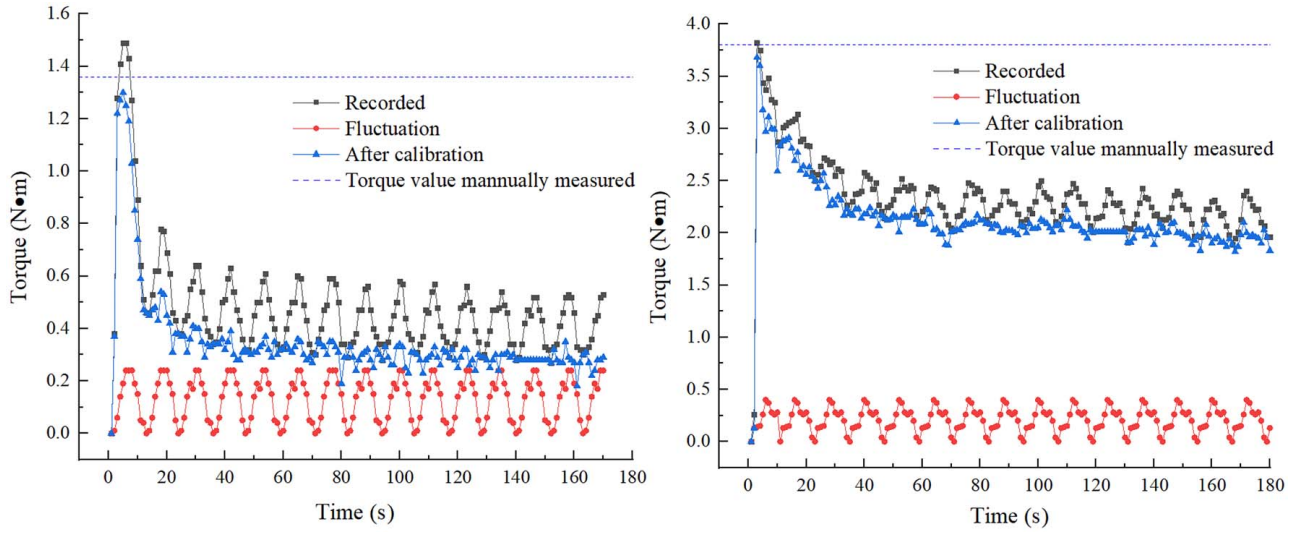

Fig. 6. Typical time history torque curves, left plate shear test, and right vane shear test.

Int. J. Geomech., 2025, 25(2): 04024341

Downloaded from ascelibrary.org by Technische Universiteit Delft on 12/23/24. Copyright ASCE. For personal use only; all rights reserved.

Test Results

Influence of Water Content

Fig. 7 shows the shear and tangential adhesion strengths of sands with various water contents that were tested at various rotation speeds. The peak values first increased with water content and then decreased to lower values. However, the residual values decreased with increasing water content. The different behavior between the peak and the residual value was probably caused by the capillary pressure. The capillary pressure increased with water content at low water content, then decreased with water content until it disappeared when the sample was saturated. Therefore, the peak value changed with the same pattern. Unlike the peak value, which was reached at the beginning of the test, the residual value was achieved after five rotations of the shear device. The sample was already sufficiently sheared at the interface; therefore, the influence of the capillary pressure no longer dominated.

For the peak values of Sands 1 and 2, the shear strength at a water content lower than 10% was quite comparable, because water will first fill in the fine voids. The grain size distribution in Sands 1 and 2 was close for particles smaller than 0.25 mm. For water contents between 10% and 20%, Sand 2 was finer for particles larger than 0.25 mm. This led to a smaller capillary tube diameter inside the soil, higher capillary pressure, and higher shear strength. Sand 3 was the finest; therefore, the maximum shear strength reached was the highest among all sands that were tested. The influence of capillary pressure disappeared when the sand was saturated at a water content of 25%; therefore, the shear strength that was measured in the three sands was comparable.

Ratio between Tangential Adhesion Strength and Shear Strength

Fig. 8 shows the ratio between the tangential adhesion and shear strengths (ratio α). For all three sands, ratio α decreased with increasing water content. The low ratio α at higher water content indicated that when tunneling in sandy soils, the pressure gradient along the screw conveyor should be paid attention because, with increasing water content, the decreasing ratio α made the reduction in the tangential adhesion strength greater than that of the shear strength. The low tangential adhesion strength at a high water content made it difficult to establish a pressure gradient along the screw conveyor. With this low-pressure gradient, the pressure in the excavation chamber had to be low to ensure zero pressure at the screw conveyor outlet. This low pressure could make it hard to create a stable tunnel face. For water content lower than 25%, the ratio α values for all three sands were higher than 0.35; the results for Sand 1 show that the ratio α tended to be stable after 0.35 was reached, which agreed well with the range of 0.4–1.0 described in Merritt and Mair (2008).

Ratio between Peak and Residual Values

The ratio between the peak and residual values is defined as ratio β and is shown in Fig. 9. This figure shows that the value of ratio β was between one and two for all sands at a water content of 0% and increased to the maximum values at water contents of 10%, 15%, and 20% for Sands 1, 2, and 3, respectively. Then, ratio β decreased to between two and three at a water content of 25% for Sands 1 and 2. For Sand 3, the value decreased to between three and four. In addition, Fig. 9 shows that the maximum value of ratio β could be higher than five; therefore, it is important to test and use residual values in the tunneling area, because the difference between the peak and residual values could be significant.

Influence of Rotation Speed

This section shows the influence of rotation speeds on the shear and tangential adhesion strengths, Ratio α, and Ratio β. To plot the results with fewer data points, the average values for sands with water contents from 0% to 25% were analyzed instead of individual values. The standard deviations were not plotted, because the water content had a significant influence on the test results, which made the plot of the standard deviations less meaningful. In addition, the large deviations could make the data points difficult to distinguish.

The influence of rotation speeds on the shear and tangential adhesion strengths is shown in Fig. 10. The shear and tangential adhesion strengths increased with the rotation speed; however, the increase was very limited. A possible explanation is that the rotation speeds that were selected in this paper were much higher than the typical rotation speed of laboratory vane shear tests, which is between 60°/min and 90°/min (ASTM D4648; ASTM 2016). The remarkably high rotation speed reduced the influence of the rotation speeds on shear strengths, because the lowest rotation speed was already high enough.

The influence of rotation speed on the ratio α is shown in Fig. 11. Because the tangential adhesion and shear strengths increased slightly with the rotation speed, the ratio α (ratio between the tangential adhesion and shear strengths) remained relatively constant despite the change in the rotation speed. The influence of the rotation speed on the ratio β is shown in Fig. 12, which shows that with peak and residual values increased with rotation speed, the ratio β (ratio between the peak and residual values) remained relatively constant despite the change in rotation speed.

Influence of Tested Sands

The results in the previous section show that the influence of the rotation speed on the test results was limited. Therefore, the influence of the tested sands was observed by studying the average values of the shear and tangential adhesion strengths, ratio α, and ratio β at various rotation speeds.

Fig. 13 shows the shear and tangential adhesion strengths of sands that were tested at various water contents, which were averaged over different rotation speeds. The shear and tangential adhesion strengths of Sand 1 were the lowest in most scenarios, and Sand 3 had the highest values. At a water content of 0%, even the residual values of Sands 2 and 3 were higher than the peak values of Sand 1. This might be because Sand 1 was the coarsest, and Sand 3 was the finest in the sands tested. In addition, the standard deviations decreased with increasing water content.

Fig. 14 shows the average values and standard deviations of the ratio α and ratio β of the tested sands at various water contents. This figure shows that the ratio α remained relatively constant at low water content and then decreased with water content in all the tested sands. This might be because the ratio α indicates the friction behavior between the metal and the sand, which is more sensitive to the water content. The trend in ratio α and the results shown in Fig. 7 agree with the results of Rostami et al. (2012), where the abrasion first increased and then decreased with water content. Sand 3 had the highest values for all water contents, and Sand 1 had the lowest values, because finer sand has closer contact between the metal and the sand, which increases the friction. The conclusions of Hamzaban et al. (2020) show a similar trend, where the influence of

Downloaded from ascelibrary.org by Technische Universiteit Delft on 12/23/24. Copyright ASCE. For personal use only; all rights reserved.

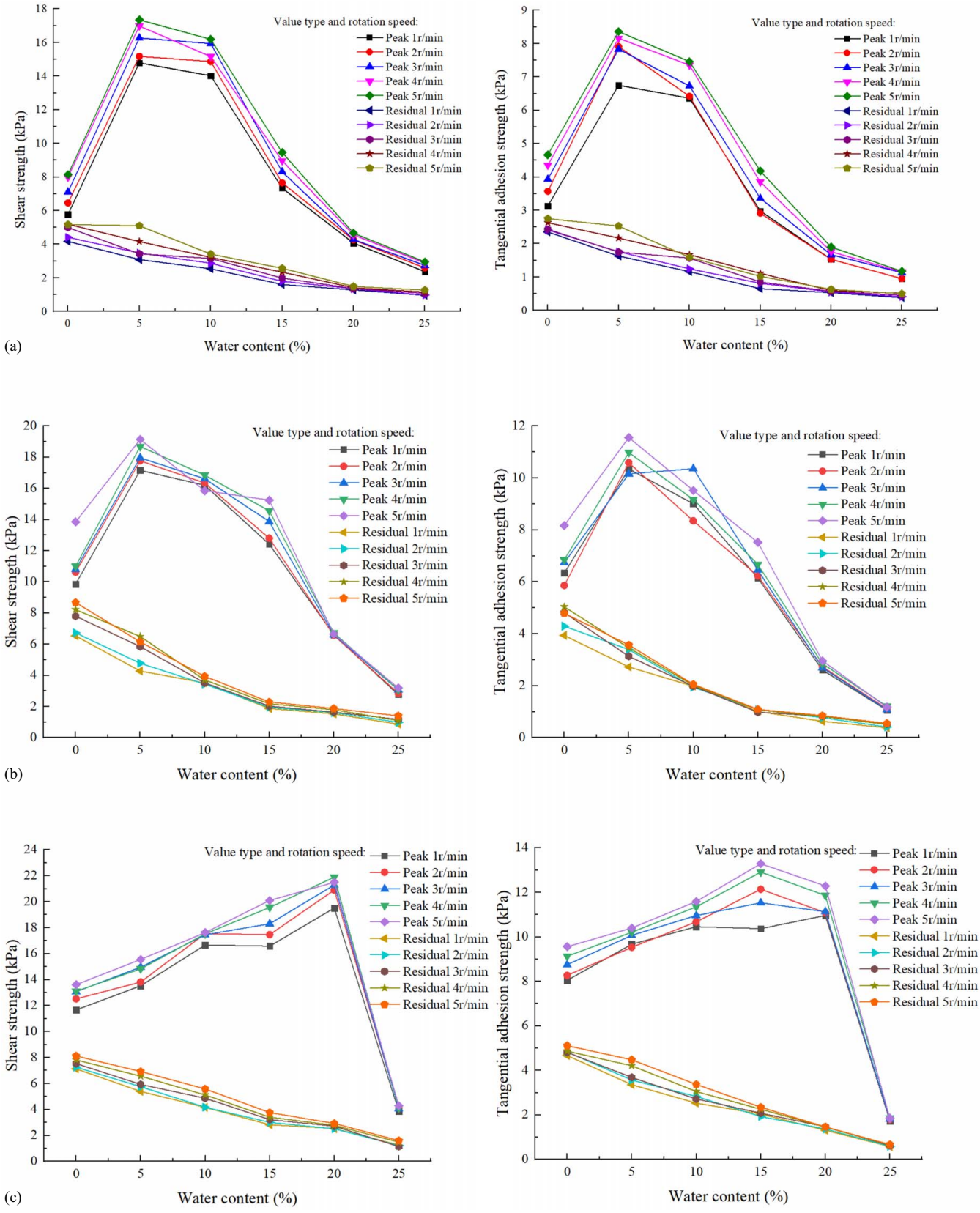

Fig. 7. Shear strengths and tangential adhesion strengths with changing water content: (a) Sand 1; (b) Sand 2; and (c) Sand 3.

confining pressure on friction is less obvious in fine soil, because the soil particles are already in close contact with the metal at low confining pressures. In addition, the ratio α values of the peak and residual values were quite similar.

The ratio β for all sands first increased to a peak value and then decreased to values of approximately three. The peak ratio β value of Sand 3 was the highest, and that of Sand 1 was the lowest. This was because the peak values increased to maximum values at low

Int. J. Geomech., 2025, 25(2): 04024341

Downloaded from ascelibrary.org by Technische Universiteit Delft on 12/23/24. Copyright ASCE. For personal use only; all rights reserved.

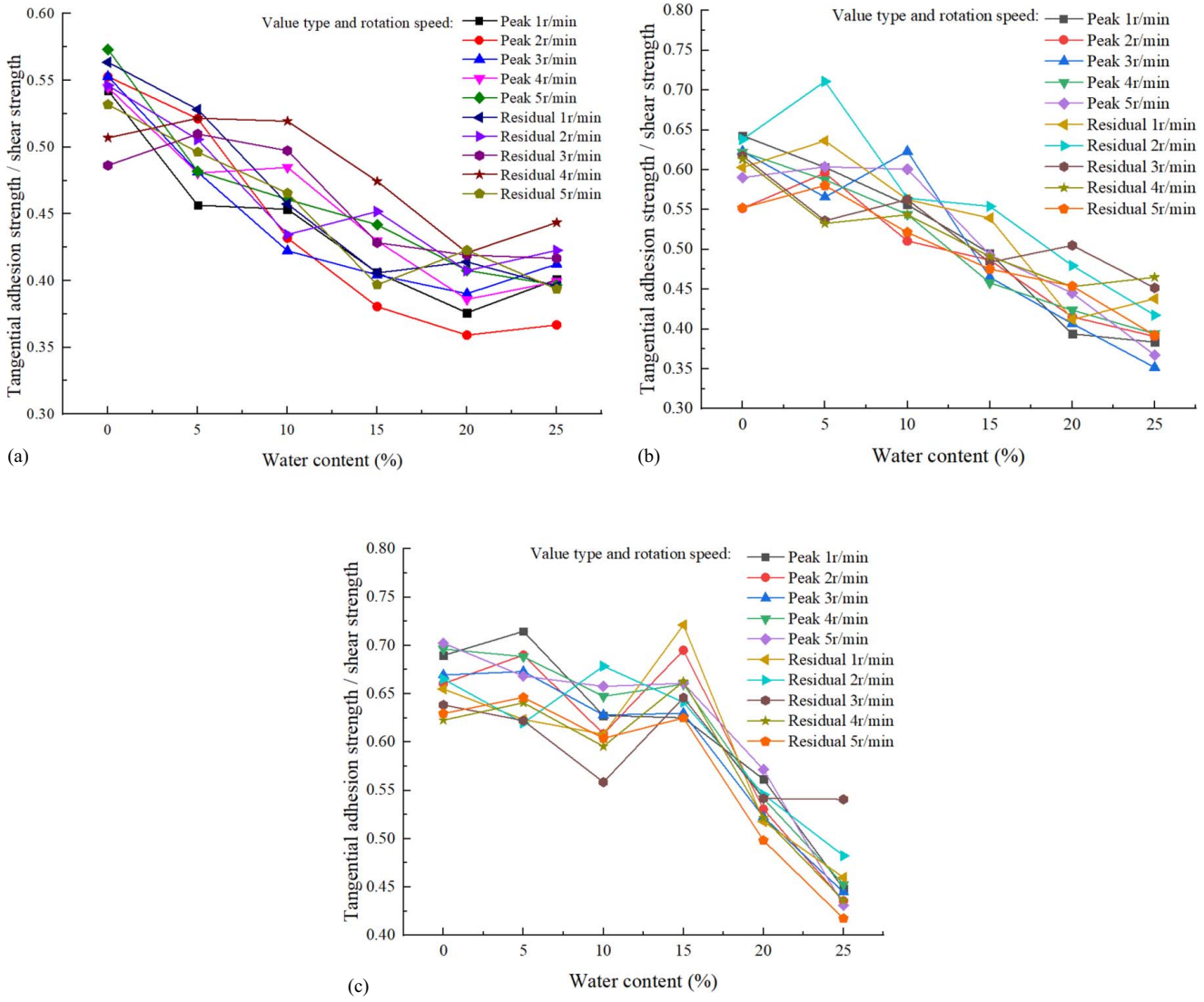

Fig. 8. Ratio α with changing water content: (a) Sand 1; (b) Sand 2; and (c) Sand 3.

water contents, and the residual values constantly decreased with the water content, as shown in Fig. 7.

The test results for all tested sands in Fig. 14 show that Sand 1 had the lowest shear and tangential adhesion strengths and ratio α. This indicates that the pressure gradient along the screw conveyor could be hard to establish when tunneling in coarse sands. For fine sands, the shear strength and ratio α were relatively higher, and the pressure gradient could be easier to establish; however, the tool abrasion could be serious. In addition, the value of ratio β that was tested in Sand 3 could be up to eight, which indicated that it was necessary to ensure that the residual values were used during the design and numerical simulation of tunneling in fine sands, because the differences between the peak and residual values were quite large.

Time Required to Reach Peak and Residual Values

Fig. 15 shows the time and rotations that are required to reach the peak values during the vane and plate shear tests. This figure shows that the time required to reach the peak values gradually decreased with increasing rotation speed for the vane and plate shear tests. In addition, Fig. 15 shows that vane shear tests reached the peak values faster than the plate shear tests. By changing the vertical axis from time to rotation, all vane shear tests reached peak values within 0.17, and all plate shear tests reached peak values between 0.25 and 0.55 r. The water content, rotation speed, and test type have very limited influence on the rotations that are required to reach peak values.

Some typical time history torque curves before calibration are shown in Fig. 16. All curves shown were obtained from tests in Sand 2 with a water content of 5%. This figure shows that the shape of the vane and plate shear curves remained the same despite the change in the rotation speed. The vane shear tests reached peak values faster than the plate shear tests; however, the plate shear tests reached the residual values faster. All curves reached a relatively stable value after five rotations.

Discussions

The results in this paper have some practical meaning for shield tunneling. The maximum value of the ratio between the peak and residual values (ratio β) was higher in finer sands, and the

Downloaded from ascelibrary.org by Technische Universiteit Delft on 12/23/24. Copyright ASCE. For personal use only; all rights reserved.

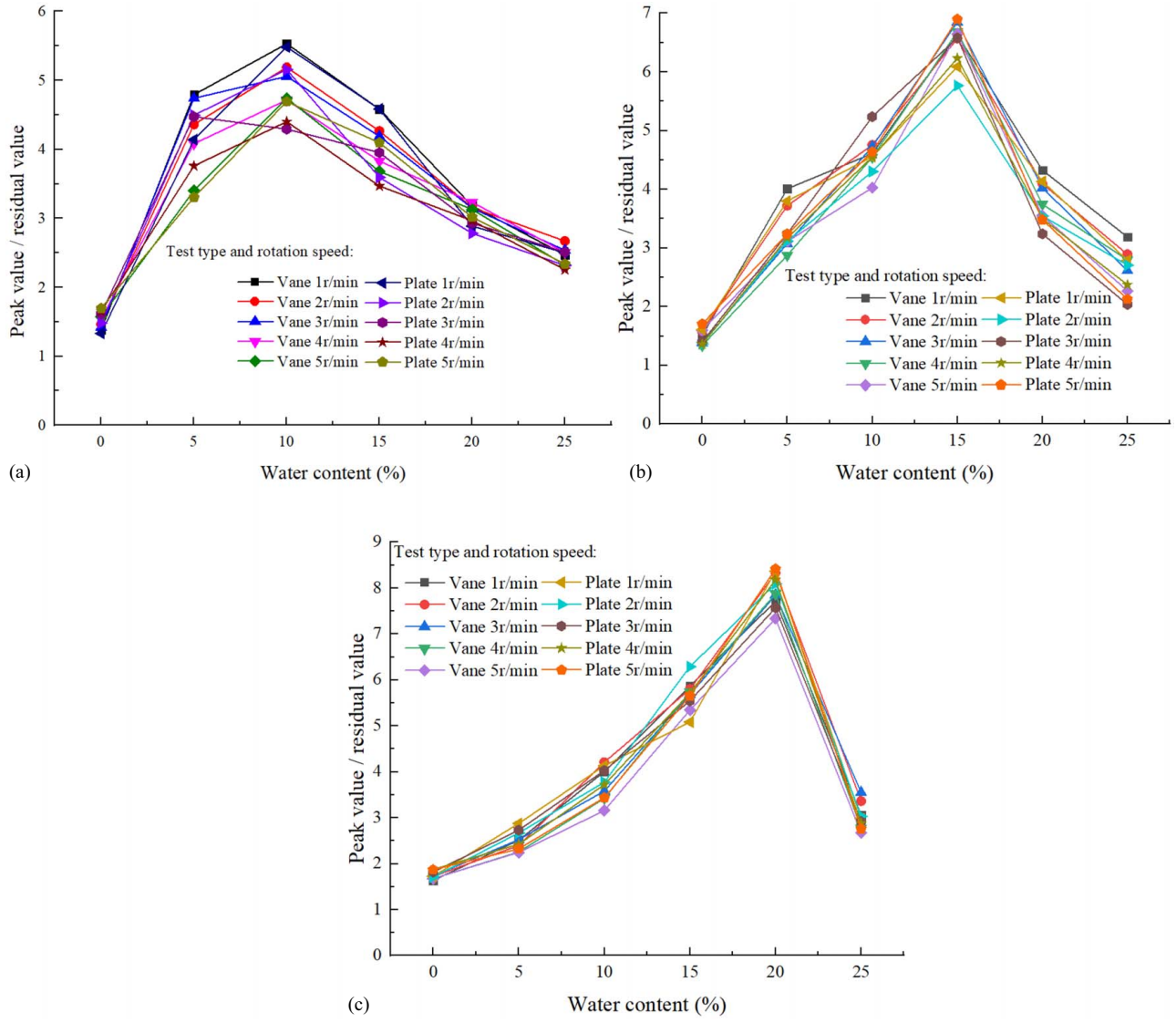

Fig. 9. Ratio β with changing water content: (a) Sand 1; (b) Sand 2; and (c) Sand 3.

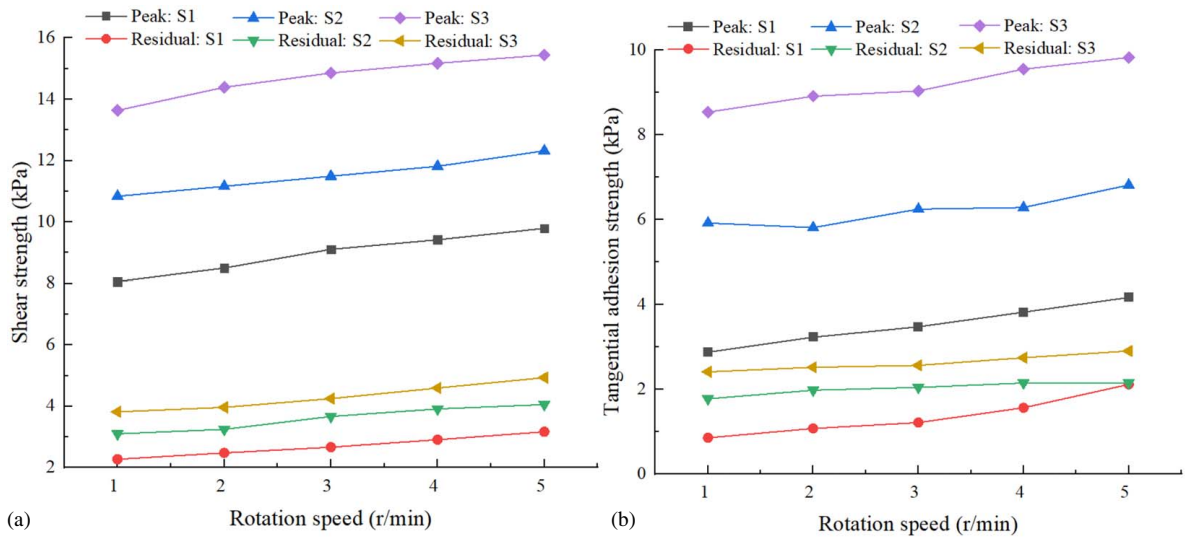

Fig. 10. (a) Average shear strength; and (b) tangential adhesion strength with changing rotation speed at water contents 0%–25%, S1, S2 and S3 refer to sands tested.

Downloaded from ascelibrary.org by Technische Universiteit Delft on 12/23/24. Copyright ASCE. For personal use only; all rights reserved.

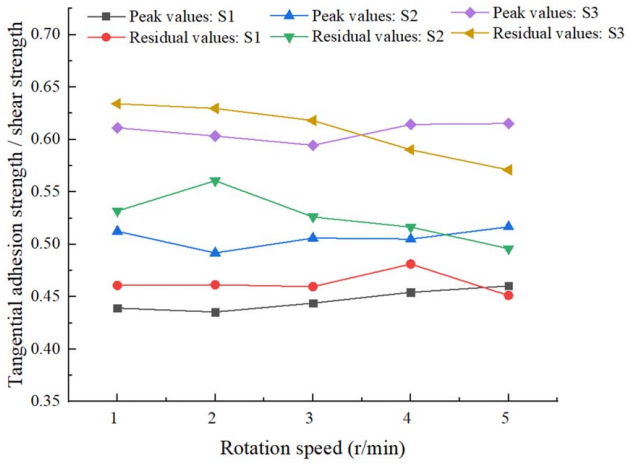

Fig. 11. Ratio α (average values of sands with water content 0%–25%) with changing rotation speed.

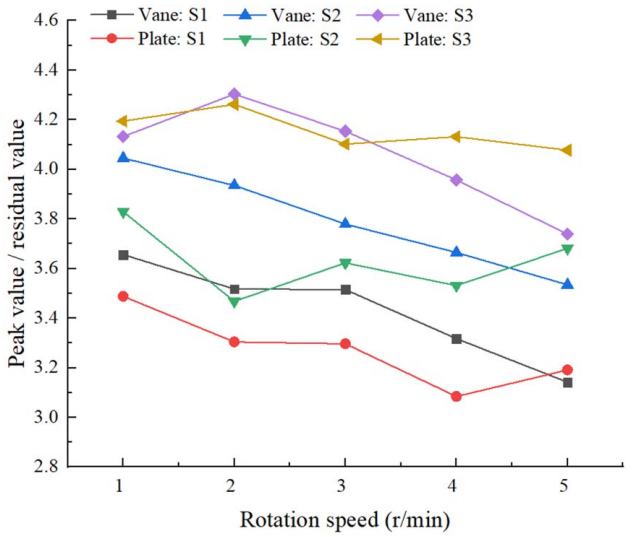

Fig. 12. Ratio β (average values of sands with water content 0%–25%) with changing rotation speed.

maximum value in this paper was over eight. During shield tunneling, because the cutterhead and crew conveyor constantly rotate, it is important to use the residual value to evaluate the abrasion of the cutter, and the pressure gradient of the screw conveyor, or the abrasion and pressure gradient will be overevaluated. In addition, after the shield machine stops for segment ring building, when the shield machine starts again, the torque required will probably be higher than the torque during constant tunneling, because the peak values should be used in this scenario.

The results in this paper show that the ratio between the tangential adhesion and shear strengths (ratio α) decreased with water content, and the ratio was lower in coarser sands. When the shield machine tunnels in sand layers with a high water content or in sand layers under the water level, the water intrusion risk in the screw conveyor could be high. The high water content reduces the tangential adhesion strength and ratio α, which leads to a low-pressure gradient along the screw conveyor. To avoid this water intrusion risk, the valve at the end of the screw conveyor should be partly closed to increase the total pressure drop. In addition, when tunneling in fine sands with limited water content, the tool abrasion could be serious due to the high shear strength and ratio α.

During shield tunneling in sand, foam is usually injected at the cutterhead to decrease the permeability of the foam–sand mixture, decrease the abrasion of the cutting tools, and decrease the torque that is required during the cutterhead rotation. Future studies should be performed with the foam–sand mixture to make the study closer to reality. In foam-conditioned sand, the void ratio is usually higher than the maximum void ratio of the sand to ensure the efficiency of soil conditioning. The high void ratio decreased the shear and tangential adhesion strengths that were measured. Therefore, the device that was described in this paper could have some advantages in future studies, because it has a higher accuracy.

However, in most shield tunneling scenarios, sand is under confining pressures. The significance of the high accuracy in this paper becomes less meaningful, because the values that were being measured were large. In addition, whether the device that was described in this paper could operate smoothly with high accuracy under confining pressures remains unclear.

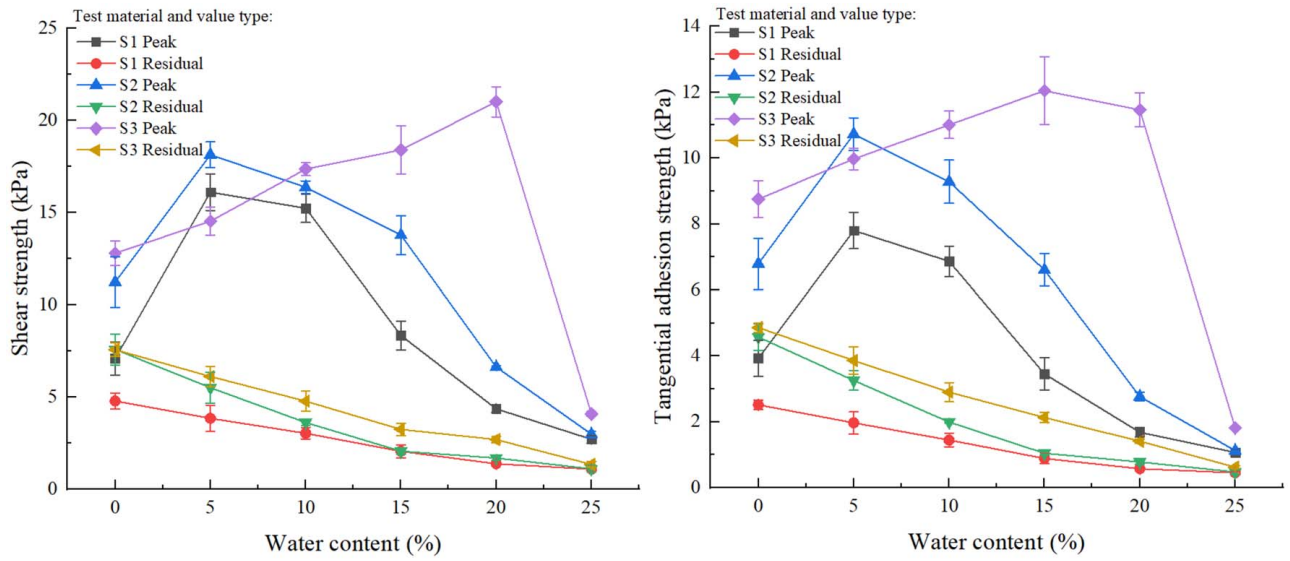

Fig. 13. Shear strengths and tangential adhesion strengths of various sands.

Downloaded from ascelibrary.org by Technische Universiteit Delft on 12/23/24. Copyright ASCE. For personal use only; all rights reserved.

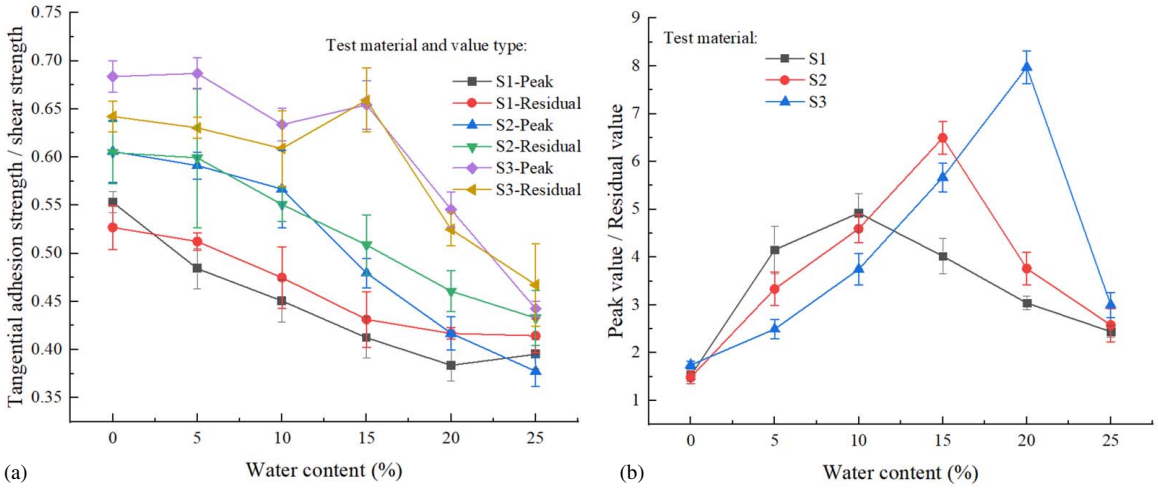

Fig. 14. Showing: (a) ratio α: and (b) ratio β of various sands.

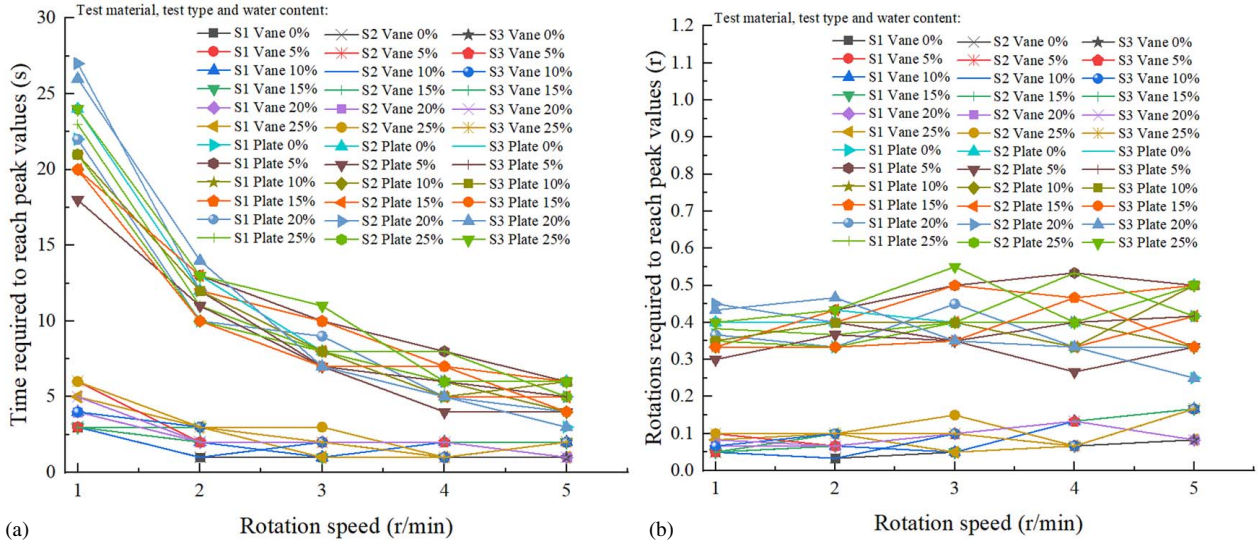

Fig. 15. Showing: (a) time; and (b) rotations required to reach peak values.

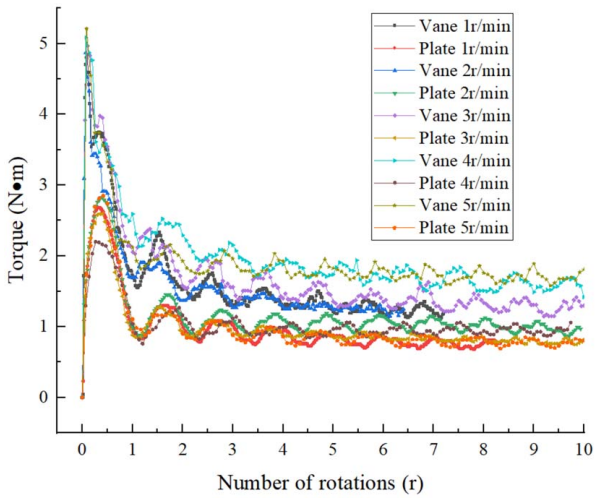

Fig. 16. Typical time history curves for vane and plate shear tests (before correction).

Conclusions

A new vane and plate shear test device was built, which could increase the accuracy of measurements by quantifying and eliminating the influence of torque fluctuation. The new device enabled the measurement of the shear and tangential adhesion strengths at atmospheric pressure, together with the study of ratios α and β, which addressed the knowledge gap. Some key conclusions could be drawn from the numerous tests that were performed in this paper.

1. The peak values of the shear and tangential adhesion strengths first increased to a maximum value and then decreased with water content. The residual values decreased with increasing water content.
2. The shear strength reached its peak value faster than the tangential adhesion strength. In this paper, the peak shear strength appears after 0.1 revolution (r), and the peak tangential adhesion strength appears after 0.4 r. However, the shear and tangential adhesion strengths approached residual values after 5 r.

Int. J. Geomech., 2025, 25(2): 04024341

Downloaded from ascelibrary.org by Technische Universiteit Delft on 12/23/24. Copyright ASCE. For personal use only; all rights reserved.

3. The ratio α decreased with increasing water content. For sands that were tested in this paper, the minimum ratio α was approximately 0.4, which appeared at a water content of 25%. The ratio β increased to the maximum value and then decreased with water content. The maximum ratio β in this paper was eight.
4. In the range of 1–5 r/min, the influence of rotation speed on the shear and tangential adhesion strengths, ratio α, and ratio β was rather limited.
5. The shear and tangential adhesion strengths, ratio α, and the maximum value of ratio β were higher in finer sands.

Although the conclusions in this paper could have some practical meaning, further research is required to make this paper closer to tunneling reality. In future research, tests will be performed with a foam–sand mixture at atmospheric pressure and with confining pressure applied.

Data Availability Statement

Some or all data, models, or codes that support the findings of this study are available from the corresponding author upon reasonable request.

Acknowledgments

The first author would like to acknowledge funding from the Special Research Fund from Ghent University, together with the scholarship that was funded by the China Scholarship Council. This work was supported by the National Natural Science Foundation of China (52078428), the Sichuan Outstanding Young Science and Technology Talent Project (2020JDJQ0032), and the 111 Project (B21011).

References

ASTM. 2016. *Standard test method for laboratory miniature vane shear test for saturated fine-grained clayey soil*. ASTM D4648. West Conshohocken, PA: ASTM.

Avunduk, E., H. Copur, S. Tolouei, D. Tumac, C. Balci, N. Bilgin, and A. Shaterpour–Mamaghani. 2021. "Possibility of using torvane shear testing device for soil conditioning optimization." *Tunnelling Underground Space Technol.* 107: 103665. https://doi.org/10.1016/j.tust.2020.103665.

Barzegari, G., M. Tirkhooni, and A. Khabbazi. 2020. "Experimental assessment of clayey layers for clogging of TBM in Tabriz subway lines, Iran." *Tunnelling Underground Space Technol.* 105: 103560. https://doi.org/10.1016/j.tust.2020.103560.

Bezuijen, A., T. Dang, and G. Meschke. 2022. "Asymmetric pressure distribution in EPB shields: Evaluation of measurements and numerical simulations." In *Geotechnical aspects of underground construction in soft ground*. 2nd ed., edited by M. Elshafie, G. Viggiani, and R. Mair, 226–233. London: CRC Press.

Bezuijen, A., and A. Talmon. 2014. "Soil pressures at the cutting wheel and the pressure bulkhead of an EPB-shield." In *Proc., 8th Int. Symp. on Geotechnical Aspects of Underground Construction in Soft Ground (IS-Seoul)*, edited by C. Yoo, S.-W. Park, B. Kim, and H. Ban, 523–529. Boca Raton, FL: CRC Press.

Bezuijen, A., A. Talmon, J. Joustra, and B. Grote. 2006. "Pressure gradients and muck properties at the face of an EPB." In *Tunnelling. A decade of progress. GeoDelft 1995–2005*, edited by A. Bezuijen and H. van Lottum, 43–49. London, UK: Taylor & Francis.

Broms, B. B., and H. Bennermark. 1967. "Stability of clay at vertical opening." *J. Soil Mech. Found. Div.* 93 (1): 71–94. https://doi.org/10.1061/JSFEAQ.0000946.

Chen, J.-N., X. Ren, H. Xu, C. Zhang, and L. Xia. 2022a. "Effects of grain size and moisture content on the strength of geogrid-reinforced sand in direct shear mode." *Int. J. Geomech.* 22 (4): 04022006. https://doi.org/10.1061/(ASCE)GM.1943-5622.0002309.

Chen, Z., A. Bezuijen, Y. Fang, K. Wang, and R. Deng. 2022b. "Experimental study and field validation on soil clogging of EPB shields in completely decomposed granite." *Tunnelling Underground Space Technol.* 120: 104300. https://doi.org/10.1016/j.tust.2021.104300.

Dzuy, N. Q., and D. V. Boger. 1985. "Direct yield stress measurement with the vane method." *J. Rheol.* 29 (3): 335–347. https://doi.org/10.1122/1.549794.

Feinendegen, M., M. Ziegler, G. Spagnoli, T. Fernández-Steeger, and H. Stanjek. 2010. "A new laboratory test to evaluate the problem of clogging in mechanical tunnel driving with EPB-shields." In *Proc., ISRM Int. Symp. - EUROCK 2010-2097*, 429–432. Lausanne, Switzerland: ISRM.

Gharahbagh, E. A., T. Qiu, and J. Rostami. 2013. "Evaluation of granular soil abrasivity for wear on cutting tools in excavation and tunneling equipment." *J. Geotech. Geoenviron. Eng.* 139 (10): 1718–1726. https://doi.org/10.1061/(ASCE)GT.1943-5606.0000897.

Gharahbagh, E. A., J. Rostami, and A. Palomino. 2011. "New soil abrasion testing method for soft ground tunneling applications." *Tunnelling Underground Space Technol.* 26 (5): 604–613. https://doi.org/10.1016/j.tust.2011.04.003.

Gharahbagh, E. A., J. Rostami, and K. Talebi. 2014. "Experimental study of the effect of conditioning on abrasive wear and torque requirement of full face tunneling machines." *Tunnelling Underground Space Technol.* 41: 127–136. https://doi.org/10.1016/j.tust.2013.12.003.

Hamzaban, M.-T., N. R. S. Mohammadi, and P. D. Jakobsen. 2020. "The effect of the particle size distribution curve on the abrasivity of non-cohesive soils in LCPC test." *Tunnelling Underground Space Technol.* 105: 103573. https://doi.org/10.1016/j.tust.2020.103573.

Ke, L., Y. Gao, D. Li, Y. Zhang, J. Zhang, and J. Ji. 2023. "An experimental study on monotonic shear behavior of the interface between fine sea sand and steel." *Int. J. Geomech.* 23 (1): 06022034. https://doi.org/10.1061/(ASCE)GM.1943-5622.0002615.

Lee, H., J. Kwak, J. Choi, B. Hwang, and H. Choi. 2022. "A lab-scale experimental approach to evaluate rheological properties of foam-conditioned soil for EPB shield tunnelling." *Tunnelling Underground Space Technol.* 128: 104667. https://doi.org/10.1016/j.tust.2022.104667.

Liu, P., S. Wang, Y. Shi, J. Yang, J. Fu, and F. Yang. 2019. "Tangential adhesion strength between clay and steel for various soil softnesses." *J. Mater. Civ. Eng.* 31 (5): 04019048. https://doi.org/10.1061/(ASCE)MT.1943-5533.0002680.

Meng, Q., F. Qu, and S. Li. 2011. "Experimental investigation on visco-plastic parameters of conditioned sands in earth pressure balance shield tunneling." *J. Mech. Sci. Technol.* 25: 2259–2266. https://doi.org/10.1007/s12206-011-0611-9.

Merritt, A., and R. Mair. 2008. "Mechanics of tunnelling machine screw conveyors: A theoretical model." *Géotechnique* 58 (2): 79–94. https://doi.org/10.1680/geot.2008.58.2.79.

MHURD (Ministry of Housing and Urban-Rural Development of the People's Republic of China). 2019. *Standard for geotechnical testing method*. GB/T 50123. Beijing: National Standardization Administration of China.

Mori, L., M. Mooney, and M. Cha. 2018. "Characterizing the influence of stress on foam conditioned sand for EPB tunneling." *Tunnelling Underground Space Technol.* 71: 454–465. https://doi.org/10.1016/j.tust.2017.09.018.

Peila, D., A. Picchio, D. Martinelli, and E. D. Negro. 2016. "Laboratory tests on soil conditioning of clayey soil." *Acta Geotech.* 11 (5): 1061–1074. https://doi.org/10.1007/s11440-015-0406-8.

Rostami, J., E. A. Gharahbagh, A. M. Palomino, and M. Mosleh. 2012. "Development of soil abrasivity testing for soft ground tunneling using shield machines." *Tunnelling Underground Space Technol.* 28: 245–256. https://doi.org/10.1016/j.tust.2011.11.007.

Shi, J., Y. Xiao, J. A. H. Carraro, H. Li, H. Liu, and J. Chu. 2023. "Anisotropic small-strain stiffness of lightly biocemented sand

Downloaded from ascelibrary.org by Technische Universiteit Delft on 12/23/24. Copyright ASCE. For personal use only; all rights reserved.

considering grain morphology." *Géotechnique* 1–14. https://doi.org/10.1680/jgeot.22.00350.

Talmon, A., and A. Bezuijen. 2006. "Muck discharge by the screw conveyor of an EPB tunnel boring machine." In *Tunnelling. A decade of progress. GeoDelft 1995-2005*, edited by A. Bezuijen and H. van Lottum, 165–170. London, UK: Taylor & Francis.

Tang, S.-H., X.-P. Zhang, Q.-S. Liu, W.-Q. Xie, H.-J. Wang, X.-F. Li, and X.-Y. Zhang. 2022. "New soil abrasion testing method for evaluating the influence of geological parameters of abrasive sandy ground on scraper wear in TBM tunneling." *Tunnelling Underground Space Technol.* 128: 104604. https://doi.org/10.1016/j.tust.2022.104604.

Ukritchon, B., K. Yingchaloenkitkhajorn, and S. Keawsawasvong. 2017. "Three-dimensional undrained tunnel face stability in clay with a linearly increasing shear strength with depth." *Comput. Geotech.* 88: 146–151. https://doi.org/10.1016/j.compgeo.2017.03.013.

Vinai, R., C. Oggeri, and D. Peila. 2008. "Soil conditioning of sand for EPB applications: A laboratory research." *Tunnelling Underground Space Technol.* 23 (3): 308–317. https://doi.org/10.1016/j.tust.2007.04.010.

Wang, S., P. Liu, Q. Hu, and J. Zhong. 2020. "Effect of dispersant on the tangential adhesion strength between clay and metal for EPB shield tunnelling." *Tunnelling Underground Space Technol.* 95: 103144. https://doi.org/10.1016/j.tust.2019.103144.

Wang, S., P. Liu, J. Zhong, Z. Ni, and T. Qu. 2022. "Influence factors and calculation model of the adhesion strength of clayey soil for EPB shield tunnelling." *Transp. Saf. Environ.* 4 (3): tdac012. https://doi.org/10.1093/tse/tdac012.

Wang, S., T. Qu, Y. Fang, J. Fu, and J. Yang. 2019. "Stress responses associated with earth pressure balance shield tunneling in dry granular ground using the discrete-element method." *Int. J. Geomech.* 19 (7): 04019060. https://doi.org/10.1061/(ASCE)GM.1943-5622.0001434.

Wang, S., Z. Zhou, P. Liu, Z. Yang, Q. Pan, and W. Chen. 2023. "On the critical particle size of soil with clogging potential in shield tunneling." *J. Rock Mech. Geotech. Eng.* 15 (2): 477–485. https://doi.org/10.1016/j.jrmge.2022.05.010.

Wilson, D. W., A. J. Abbo, S. W. Sloan, and A. V. Lyamin. 2013. "Undrained stability of a square tunnel where the shear strength increases linearly with depth." *Comput. Geotech.* 49: 314–325. https://doi.org/10.1016/j.compgeo.2012.09.005.

Xiao, Y., H. Li, J. Shi, J. Hu, L. Zhang, and H. Liu. 2023. "Effect of particle size on small strain stiffness of biotreated sands." *Transp. Geotech.* 41: 101027. https://doi.org/10.1016/j.trgeo.2023.101027.

Yang, Y., X. Li, and X. Li. 2018. "Shear strength and compression coefficient for conditioned sand subjected to earth chamber stress levels." *Adv. Mater. Sci. Eng.* 2018 (1): 1759151. https://doi.org/10.1155/2018/1759151.

Zhang, C., W. Li, W. Zhu, and Z. Tan. 2020. "Face stability analysis of a shallow horseshoe-shaped shield tunnel in clay with a linearly increasing shear strength with depth." *Tunnelling Underground Space Technol.* 97: 103291. https://doi.org/10.1016/j.tust.2020.103291.

Zhong, J., S. Wang, and T. Qu. 2023. "Undrained vane shear strength of sand-foam mixtures subjected to different shear rates." *J. Rock Mech. Geotech. Eng.* 15 (6): 1591–1602. https://doi.org/10.1016/j.jrmge.2022.11.002.

Zumsteg, R., M. Plötze, and A. M. Puzrin. 2013. "Reduction of the clogging potential of clays: New chemical applications and novel quantification approaches." *Géotechnique* 63 (4): 276–286. https://doi.org/10.1680/bcmpge.60531.004.

Zumsteg, R., and A. M. Puzrin. 2012. "Stickiness and adhesion of conditioned clay pastes." *Tunnelling Underground Space Technol.* 31: 86–96. https://doi.org/10.1016/j.tust.2012.04.010.

Downloaded from ascelibrary.org by Technische Universiteit Delft on 12/23/24. Copyright ASCE. For personal use only; all rights reserved.